Glucose-Induced Conformational Changes in Glucokinase Mediate Allosteric Regulation: Transient Kinetic Analysis

Vladi V. Heredia,[‡] Jim Thomson,[‡] David Nettleton,[§] and Shaoxian Sun*[,‡]

Biochemical Pharmacology, La Jolla Laboratory, Pfizer Global Research and Development, San Diego, California 92121, and Lead Assessment Team, Pfizer Global Research and Development, Groton, Connecticut 06340

Received February 6, 2006; Revised Manuscript Received April 5, 2006

ABSTRACT: The transient kinetics of glucose binding to glucokinase (GK) was studied using stopped-flow fluorescence spectrophotometry to investigate the underlying mechanism of positive cooperativity of monomeric GK with glucose. Glucose binding to GK was shown to display biphasic kinetics that fit best to a reversible two-step mechanism. GK initially binds glucose to form a transient intermediate, namely, E*·glucose, followed by a conformational change to a catalytically competent E·glucose complex. The microscopic rate constants for each step were determined as follows: on rate k_1 of 557 M^{-1} s^{-1} and off rate k_{-1} of 8.1 s^{-1} for E*·glucose formation, and forward rate k_2 of 0.45 s^{-1} and reverse rate k_{-2} of 0.28 s^{-1} for the conformational change from E*·glucose to E·glucose. These results suggest that the enzyme conformational change induced by glucose binding is a reversible, slow event that occurs outside the catalytic cycle (k_{cat} = 38 s^{-1}). This slow transition between the two enzyme conformations modulated by glucose likely forms the kinetic foundation for the allosteric regulation. Furthermore, the kinetics of the enzyme conformational change was altered in favor of E·glucose formation in D_2O, accompanied by a decrease in cooperativity with glucose (Hill slope of 1.3 in D_2O vs 1.7 in H_2O). The deuterium solvent isotope effects confirm the role of the conformational change in the magnitude of glucose cooperativity. Similar studies were conducted with GK activating mutation Y214C at the allosteric activator site that is likely involved in the protein domain rearrangement associated with glucose binding. The mutation enhanced equilibrium glucose binding by a combination of effects on both the formation of E*·glucose and an enzyme conformational change to E·glucose. Kinetic simulation by KINSIM supports the conclusion that the kinetic cooperativity of GK arises from slow glucose-induced conformational changes in GK.

Glucokinase (GK[1] or hexokinase IV) is a member of the hexokinase (HK) family and catalyzes the phosphorylation of glucose to glucose 6-phosphate, the rate-limiting step in glycolysis. It serves as a glucose sensor of glucose-dependent insulin secretion in pancreatic β-cells and regulates glucose uptake and glycogen synthesis in the liver (*1*−*4*). GK plays a critical role in glucose homeostasis as evidenced by naturally occurring mutations that lead to pathogenic complications. Inactivating mutations in GK have been linked to maturity-onset diabetes of the young (MODY2), an autosomal dominant form of diabetes mellitus (*5*), while activating GK mutations lead to varying degrees of hyperinsulinemia and hypoglycemia (*6*−*8*).

Compared to other HKs, GK has unique biochemical kinetics that accounts for its role as a glucose sensor (*1*−*3*, *5*). GK has a low affinity for glucose as a substrate with a $K_{0.5}$ of ∼7 mM, which is within the physiological glucose range. The enzyme also has no direct feedback inhibition by its product glucose 6-phosphate. Although it is a monomeric enzyme, GK displays a sigmoidal saturation curve for glucose with a characteristic Hill slope of ∼1.7. The inflection point of the sigmoidal curve (4−5 mM) is close to the physiological threshold for glucose-stimulated insulin secretion in β-cells. Functionally, this positive cooperativity with glucose allows the enzyme to have increased sensitivity to fluctuations in blood glucose levels (*9*). Together, these kinetic properties enable GK to be highly responsive to glucose levels and to ensure that the glucose metabolic flux is closely tied to the glucose concentration.

The crystal structures of GK suggest that the enzyme undergoes substantial conformational changes during catalysis (Figure 1) (*10*). The degree of domain rearrangement observed in human GK induced by glucose binding is much larger than that in yeast HK and human HK type I (*11*−*13*). In addition, an allosteric site was identified in GK where a small molecule activator was bound in a cleft between the large and small domains approximately 20 Å from and opposite the glucose-binding site (*10*, *14*, *15*). Most of the GK activating mutations are located in the allosteric site. Both GK activating mutations and small molecule activators achieve the activation effects by decreasing the $K_{0.5}$ for glucose, suggesting some similar mechanistic properties in

* To whom correspondence should be addressed: Biochemical Pharmacology, La Jolla Laboratory, Pfizer Global Research and Development, 10628 Science Center Dr., San Diego, CA 92121. Phone: (858) 526-4922. Fax: (858) 526-4240. E-mail: shaoxian.sun@pfizer.com.

‡ La Jolla Laboratory.

§ Lead Assessment Team.

[1] Abbreviations: GK, glucokinase; HK, hexokinase; WT, wild-type; MODY2, maturity-onset diabetes of the young type 2; PK/LDH, pyruvate kinase/lactate dehydrogenase; PEP, phosphoenolpyruvate; DTT, dithiothreitol; TCEP, tris(2-carboxyethyl)phosphine; D_2O, deuterium oxide; SDS−PAGE, sodium dodecyl sulfate−polyacrylamide gel electrophoresis; QTOF-MS, quadrupole time-of-flight mass spectrometry; NADH, nicotinamide adenine dinucleotide hydrate; DSC, differential scanning calorimetry.

10.1021/bi060253q CCC: $33.50
Published on Web 05/26/2006

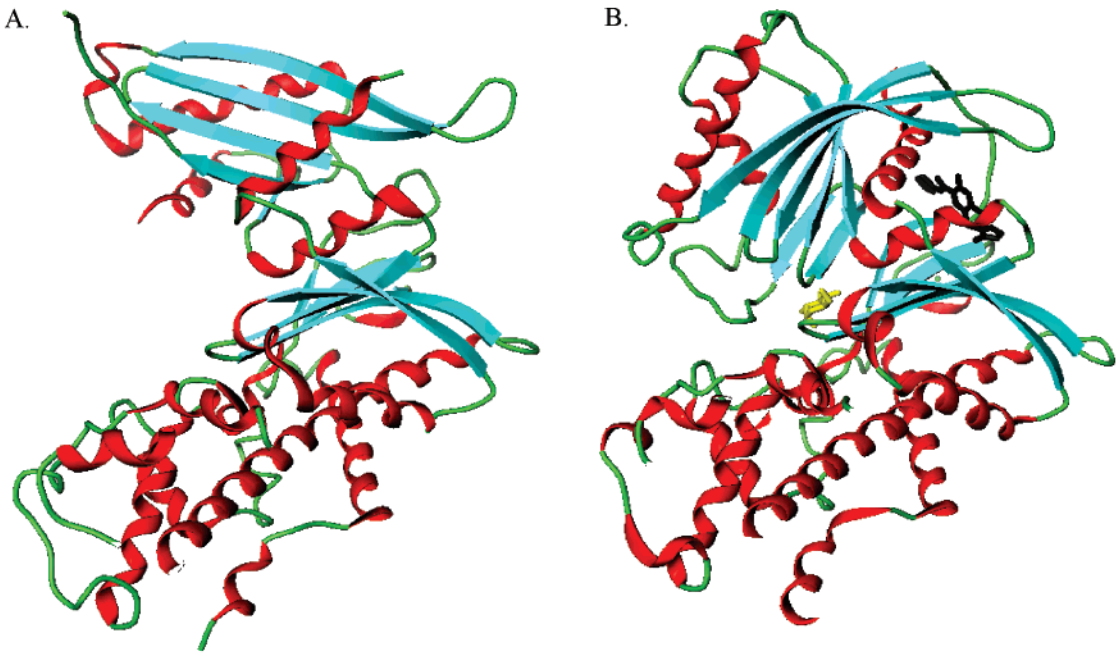

FIGURE 1: Glucokinase undergoes a large conformational change from (A) the apoenzyme form to (B) the complex form with glucose (yellow) and the activator (black). Helices, β-sheets, and flexible loops are colored red, blue, and green, respectively. The structures were adapted from the Protein Data Bank entry of Kamata et al. (*10*).

GK activation by perturbation of the allosteric site. Among the GK activating mutations, Y214C causes some of the most severe clinical symptoms of hypoglycemia and hyperinsulinemia (*8*). Structurally, Y214 has been shown to interact with a GK activator at the allosteric site and is located at the connecting region of two domains that is directly involved in enzyme conformational change upon glucose binding (*10*, *16*). It is reasonable to hypothesize that the enzyme structural changes are closely linked to the allosteric modulation of GK activity.

In this study, the kinetics of the structural transition from apo-GK to glucose-bound GK was investigated by monitoring the changes in the intrinsic protein fluorescence associated with glucose binding using stopped-flow spectrophotometry. Biphasic kinetics was observed for glucose binding, suggesting a two-step binding mechanism: initial formation of an enzyme−glucose complex followed by an enzyme conformational change. The associated microscopic rate constants were determined for this two-step mechanism, and the results showed that the enzyme conformational change is a slow step. Furthermore, GK activating mutation Y214C was studied to elucidate the relationship between the structural perturbation at the allosteric site and the biphasic kinetics, and the underlying mechanism for GK activation. Because activating GK mutations modulate enzyme activity in a manner similar to that of small molecule activators, this study provides insight into how small molecule activators may achieve their pharmacological effects. This analysis may further contribute to our understanding and the design of small molecule GK activators as potential therapeutics for the treatment of diabetes.

EXPERIMENTAL PROCEDURES

Materials. Glucose, 2-deoxyglucose, pyruvate kinase/lactate dehydrogenase (PK/LDH), phosphoenolpyruvate (PEP), dithiothreitol (DTT), tris(2-carboxyethyl)phosphine (TCEP), and ATP were obtained from Sigma. Deuterium oxide (D_2O, >99% pure), deuterium chloride, and sodium deuterioxide were also purchased from Sigma. Yeast HK was obtained from Worthington Biochemical Corp. All other reagents were ACS grade or better.

Expression and Purification of Recombinant Proteins. The cloning of human β-cell GK has been described previously (*17*). The protein was expressed in *Escherichia coli* BL21-(DE3) cells with an N-terminal hexahistidine tag. Bacterial cells were grown in 2 L cultures of 2XYT medium initially at 37 °C, containing 100 μg/mL ampicillin. Once A_{600} reached 0.6, 0.1 mM IPTG was added to induce enzyme expression overnight at 23 °C. Purification was achieved by sequential chromatography on a Ni^{2+}−nitriloacetate column and a size-exclusion column. The purity of the enzyme was verified by SDS−PAGE and QTOF-MS. Protein concentrations were determined by the method of Bradford (*18*). Homogeneous enzyme was stored in aliquots at −80 °C in a pH 7.5 buffer containing 25 mM HEPES, 50 mM NaCl, 5 mM DTT, and 5% glycerol.

The oligonucleotide primers used to generate allosteric site mutation Y214C are as follows: forward primer, GCC ACG ATG ATC TCC TGC T*GC* *T*AC GAA GAC CAT CAG TGC; and reverse primer, GCA CTG ATG GTC TTC GT*A* *GC*A GCA GGA GAT CAT CGT GGC. Underlined nucleotides indicate the site of mutation. The QuickChange site-directed mutagenesis kit (Stratagene) was used to generate the mutant, and dideoxy sequencing ensured the fidelity of the mutant constructs. A pET15b-glucokinase vector encoding the mutant was used to transform *E. coli* BL21(DE3) cells. The mutant protein was purified by the same protocol that was used for wild-type GK.

Steady-State Kinetics of Wild-Type (WT) GK and Y214C. Initial rates for GK activity were measured at 25 °C using a PK/LDH coupled assay. This coupled enzyme system was chosen over glucose-6-phosphate dehydrogenase for two

reasons. First, the ATP concentration remains constant by regeneration through the coupled reaction. Second, the product inhibition of ADP on GK, although weak, can be minimized by immediate conversion to ATP. To determine the steady-state kinetics with respect to glucose or ATP, the assay was performed using 0−50 mM glucose at a saturating concentration of 2 mM ATP, or 0−2 mM ATP at a saturating concentration of 50 mM glucose in a buffer comprised of 50 mM HEPES (pH 8.0), 3 mM $MgCl_2$, 25 mM KCl, 0.7 mM NADH, 2 mM DTT, 4 mM PEP, and 1 unit/mL PK/LDH. For 2-deoxyglucose as the substrate, 2 mM ATP was used in the assay. The assay was conducted in a 96-well plate with a final volume of 100 μL. Reactions were initiated by the addition of enzyme and monitored by the depletion of NADH at 340 nm. Under these conditions, the initial absorbance was always <1.2 OD units. A lag phase observed in the time course was allowed to pass, and the steady-state initial rate was determined using the assay time range of 200−900 s. This lag phase became negligible when the enzyme was preincubated with glucose, and the reaction was initiated by the addition of ATP. However, the order of addition of reagents did not change the initial steady-state rate. The steady-state kinetic parameters were determined by curve fitting to the Hill equation (eq 1) for glucose due to its sigmoidal kinetics, and Michaelis−Menten equation for ATP with hyperbolic kinetics using a nonlinear regression analysis program (Prism, GraphPad Inc.).

$$V = \frac{V_{max} S^h}{K_{0.5}{}^h + S^h} \quad (1)$$

where V_{max} is the maximal activity of GK, S is the glucose concentration, $K_{0.5}$ is the glucose concentration at half-maximal activity, h is the Hill slope, and V is the activity at a given glucose concentration S.

Substrate Binding to WT GK by Differential Scanning Calorimetry. Differential scanning calorimetry (DSC) was used to examine the binding of glucose or ATP to GK. DSC experiments were performed using a VP-DSC instrument from MicroCal, Inc. (Northampton, MA). The glucokinase was exhaustively dialyzed against 50 mM HEPES buffer (pH 8.0), 25 mM KCl, and 2.0 mM TCEP. The protein concentration was determined spectrophotometrically using a calculated extinction coefficient of 31 150 M^{-1} cm^{-1}, and the protein concentration used for all scans was 0.3 mg/mL. Prior to the measurements, 1.0% (v/v) DMSO was added, and the samples were degassed. GK thermal denaturation scans were performed in the absence and presence of either 100 mM glucose or 10 mM ATP with 10 mM $MgCl_2$. Scans were typically run from 20 to 70 °C at a scan rate of 90 °C/h in the passive mode. The reversibility of GK thermal denaturation was assessed by checking the reproducibility of 20−70 °C scans after cooling and rescanning of a protein sample. An aliquot of the protein was scanned to 90 °C to determine the thermal midpoint of transition (T_m) of GK under the stated conditions. A second aliquot of the protein was then heated to 50 °C (the approximate T_m as determined by the previous scan), cooled, rescanned to 70 °C, cooled, and again rescanned to 70 °C. The scans were more than 90% reproducible after heating to 50 °C but were completely irreversible after heating to 70 °C. No attempt to assess the reversibility by varying the scan speed was performed. As the thermal unfolding of GK was reversible upon heating to the thermal midpoint of the transition but not reversible after heating to a temperature sufficient to establish a post-transition baseline, only the thermal midpoint of the transition from the fitting result was reported. The data were fit using ORIGIN provided with the instrument. Background scans, collected with buffer in both the sample and reference cells, were subtracted from sample scans prior to analysis.

Equilibrium Binding Affinity for Binding of Sugar Substrates to Glucokinase. The binding of glucose or 2-deoxyglucose to GK causes an increase in the intrinsic protein fluorescence of GK, which was monitored by fluorescence spectrometry (Tecan Safire). The assay was performed in a 96-well plate with a final volume of 100 μL. The equilibrium binding affinity of glucose or 2-deoxyglucose was measured by incubating the enzyme with various concentrations of the sugar substrate. Each sample contained 19 μM enzyme in 50 mM HEPES (pH 8.0), 25 mM KCl, and 2 mM DTT at 25 °C with either 0−50 mM glucose or 0−400 mM 2-deoxyglucose. Samples were excited at 290 nm, and fluorescence emission was scanned from 305 to 400 nm (excitation and emission band-pass set at 5 nm). The maximal GK protein absorption and emission wavelengths were determined to be 290 and 330 nm, respectively. The fluorescence readout at the λ_{max} of 330 nm was corrected by subtracting the background fluorescence obtained in the absence of substrate and plotted as a function of substrate concentration S. The binding affinity (K_D) and the associated standard errors were determined by fitting the data to a binding equation using nonlinear regression analysis [fluorescence = $\text{fluorescence}_{max} S/(K_D + S)$].

Transient Kinetics of Sugar Substrate Binding As Determined by Stopped-Flow Spectrophotometry. Pre-steady-state kinetics was measured by the rapid mixing of enzyme and substrate at 25 °C using an Applied Photophysics SX.18MV stopped-flow spectrophotometer (dead time of 1 ms). Enzyme (final concentration of 5 or 10 μM) and varying concentrations of sugar substrate (final concentrations of 0.1−50 mM glucose or 10−400 mM 2-deoxyglucose) in 50 mM HEPES (pH 8.0), 25 mM KCl, and 2 mM DTT were introduced into the stopped-flow apparatus via separate syringes. Reactions were initiated by the rapid mixing of the two solutions. The change in the intrinsic enzyme fluorescence was monitored using a 320 nm cutoff filter with excitation at 290 nm. Readings were recorded on a log time scale to capture the fast phase kinetics. The kinetic time traces were analyzed using Applied Photophysics SX.18MV version 4.2 based on a robust nonlinear regression (Marquardt) algorithm. At least five traces per substrate concentration were collected, and the average was used in the curve fitting. For biphasic kinetics, the rate constants (k_{obs1} and k_{obs2}) and the amplitudes (A_1 and A_2) were determined from double-exponential fits to eq 2. Parameter C in eq 2 was a fitting variable.

$$Y = A_1 e^{-k_{obs1} t} + A_2 e^{-k_{obs2} t} + C \quad (2)$$

A similar study with yeast HK was also performed to determine its kinetics of substrate binding. A quench in protein fluorescence of HK (5−20 μM) was observed at the steady state in the presence of 0.1−1 mM glucose. However, a majority of the fluorescence change caused by glucose

Scheme 1: Model for Kinetic Partitioning in Glucokinase

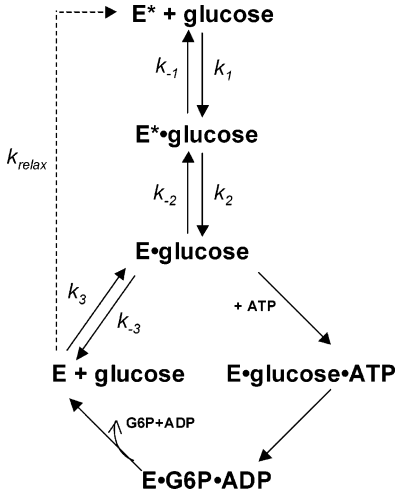

binding occurred within the dead time of the stopped-flow instrument (1 ms). Thus, the transient kinetics for binding of glucose to HK could not be well determined. The measurement limit of k_{obs} is $<1500\ s^{-1}$.

Solvent Kinetic Isotope Effects. Buffers prepared in D_2O were adjusted to the desired pD value with either sodium deuterioxide or deuterium chloride using a pH meter. Appropriate corrections were made to the meter reading according to the formula pD = meter reading + 0.4 (*19*). To maximize the deuteration of protonated amino acid residues, the enzyme was exchanged into the appropriate D_2O buffers via Centricon ultrafiltration at least five times. The enzyme was then incubated in the D_2O buffer for 4 h on ice. The buffer exchange did not result in any loss of enzyme activity.

Solvent kinetic isotope effects for glucose turnover and glucose binding were determined under identical conditions as described above in D_2O and H_2O buffers and reported using the nomenclature of Northrop (*20*) as the ratio of the parameter measured in H_2O over that in D_2O.

Kinetic Simulations. The kinetic simulation program KINSIM (*21*) was used to model the data. The aim of the simulation was to test whether the enzyme mechanism outlined in Scheme 1 and the measured rate constants of glucose binding give rise to the kinetic cooperativity of GK. Equations used in the simulation were written as described in Scheme 1 except the steps of ATP binding, phosphoryl group transfer, and product release were simplified as one step described by k_{cat}. The rate constants for each step were assigned on the basis of the experimentally determined values (k_1, k_{-1}, k_2, k_{-2}, and k_{cat}) and assumptions (k_3, k_{-3}, and k_{relax}). The delta time was set to 500 s with the integral tolerance set to 0.1. The reaction progress curves were simulated at various substrate concentrations. Steady-state initial velocities were obtained from the linear part (90−500 s) of the simulated curve. The concentration-dependent rates were fit to the Hill equation (eq 1) to obtain the Hill slope and $K_{0.5}$ for glucose or 2-deoxyglucose with GK and Y214C.

RESULTS

Steady-State Kinetics of WT GK and the Y214C Mutant. Steady-state kinetic properties of recombinant human β-cell WT GK and Y214C were determined for glucose, its analogue 2-deoxyglucose, and ATP. Results are summarized in Table 1. WT GK exhibited positive cooperativity with glucose (Hill slope of 1.7) while showing little cooperativity with 2-deoxyglucose (Hill slope of 1.1). Compared to glucose, 2-deoxyglucose was a poor substrate for WT GK with a 20-fold increase in $K_{0.5}$. For the GK activating mutation Y214C, the enhanced catalytic efficiency mainly came from a 3-fold decrease in the $K_{0.5}$ of glucose while the k_{cat} remained the same. The K_m for ATP was slightly increased for Y214C versus that for WT. The positive cooperativity with glucose observed with WT GK was nearly eliminated with GK activating mutation Y214C (Hill slope of 1.2).

Table 1: Steady-State Kinetic Parameters for WT GK and Y214C in (A) H_2O and (B) D_2O

	WT GK		Y214C
	glucose	2-deoxyglucose	glucose
	(A) H_2O		
k_{cat} (s^{-1})	38 ± 1	29 ± 1	39 ± 1
$K_{0.5}$ (mM)	7.2 ± 0.2	153 ± 19	2.2 ± 0.1
Hill slope	1.7 ± 0.1	1.1 ± 0.1	1.2 ± 0.1
K_m(ATP) (mM)	0.14 ± 0.01	ND[a]	0.23 ± 0.01
	(B) D_2O		
k_{cat} (s^{-1})	18 ± 1	20 ± 1	24 ± 1
$K_{0.5}$ (mM)	5.7 ± 0.2	80 ± 7	1.4 ± 0.1
Hill slope	1.3 ± 0.1	1.0 ± 0.1	1.1 ± 0.1
K_m(ATP) (mM)	0.18 ± 0.02	ND[a]	0.32 ± 0.01

[a] An accurate K_m(ATP) could not be determined because of limits imposed by 2-deoxyglucose solubility at saturating levels (~800 mM).

The steady-state kinetic parameters in D_2O were determined to evaluate solvent isotope effects (Table 1B). For WT GK, normal solvent isotope effects on k_{cat} were observed as 2.1 ± 0.1 and 1.4 ± 0.1 using glucose and 2-deoxyglucose as the substrate, respectively. The positive cooperativity with glucose was decreased in D_2O with a Hill slope of 1.3. For Y214C with glucose, the solvent isotope effect on k_{cat} was 1.6 ± 0.1, similar to that of WT GK.

Formation of a Binary Complex with Glucokinase and Glucose. Before binding studies for the sugar substrates with human β-cell GK were initiated, differential scanning calorimetry studies were conducted to confirm the formation of a binary complex between the enzyme and glucose in the absence of ATP. Specific binding of a substrate to protein is predicted to shift the transition temperature of protein unfolding to a greater value (*22*). The results were obtained after we subtracted a buffer−buffer reference trace, normalized them for concentration and scan rate, and removed a progressive baseline representing the contribution of the heat capacity change. These resultant traces were fit using a non-two-state model with a zero heat capacity change. The thermal midpoint of the transitions was determined to be 48.0 ± 0.1, 49.6 ± 0.1, and 48.0 ± 0.1 °C for GK alone, GK with 100 mM glucose, and GK with 10 mM ATP-$MgCl_2$, respectively. The glucose concentration used for the DSC study was approximately 20-fold greater than the glucose K_D as determined by fluorescence binding studies, while the ATP concentration was approximately 70-fold greater than the ATP K_m determined by steady-state kinetic studies. Whereas the thermal unfolding of GK in the presence of glucose produced results significantly different from those obtained in the absence of glucose, the results for the thermal unfolding of GK and the GK/ATP/$MgCl_2$ mixture were

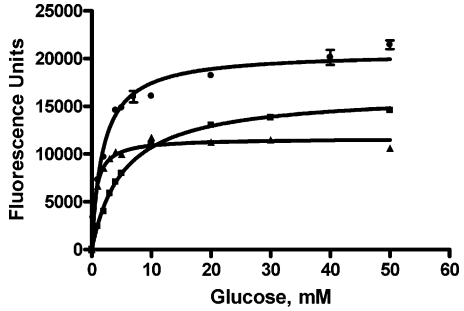

FIGURE 2: Binding isotherm for binding of glucose to WT GK (in H_2O and D_2O) and to Y214C (in H_2O): (■) WT GK in H_2O, (●) WT GK in D_2O, and (▲) Y214C in H_2O.

Table 2: Binding Affinities (K_D) and Solvent Isotope Effects (SIE) of WT GK and Y214C with Glucose and 2-Deoxyglucose

	WT GK		Y214C	
	glucose	2-deoxyglucose	glucose	2-deoxyglucose
$K_D(H_2O)$ (mM)	4.5 ± 0.2	419 ± 32	0.67 ± 0.05	96 ± 12
$K_D(D_2O)$ (mM)	1.9 ± 0.1	413 ± 34	0.87 ± 0.09	96 ± 10
SIE, $^{D_2O}K_D$	2.4 ± 0.2	1.0 ± 0.1	0.77 ± 0.13	1.0 ± 0.2

essentially indistinguishable. The addition of glucose resulted in a 1.6 °C shift in the T_m and a significant sizable increase in the enthalpy of unfolding. This result clearly demonstrated the formation of a binary complex between GK and glucose in the absence of ATP.

Equilibrium Binding Affinity of Sugar Substrates for Glucokinase. The intrinsic protein fluorescence of GK was utilized to determine binding affinities for its natural substrate glucose and the substrate analogue 2-deoxyglucose. The binding curves of glucose with WT GK and Y214C are shown in Figure 2, and the fitted results are summarized in Table 2. The glucose binding curves exhibited a hyperbolic curvature, in contrast to the sigmoidal dependence with glucose in glucose turnover for WT GK. The binding affinity of glucose for the wild-type enzyme ($K_D = 4.5$ mM) was slightly lower than the $K_{0.5}$ (7.2 mM) determined from steady-state kinetic measurements of glucose turnover. The binding study confirmed that 2-deoxyglucose was a poor substrate for WT GK with an ~100-fold weaker binding affinity ($K_D = 419$ mM). A higher binding affinity was observed when glucose binding was measured in a D_2O-solvent system ($K_D = 1.9$ mM), leading to an isotope effect of 2.4 ± 0.2. The activating Y214C mutation yielded higher binding affinities for the sugar substrates with K_D values for glucose and 2-deoxyglucose of 0.67 and 96 mM, respectively.

Transient Kinetics of Sugar Substrate Binding to Glucokinase. Previous studies characterizing GK have mainly focused on the steady-state kinetic portion of the mechanism. Such measurements are reflections of overall events and cannot distinguish between the formation and decay of individual intermediates on the reaction pathway. To determine whether glucose binding to GK consists of one event or multiple events, rapid mixing experiments were conducted to detect and analyze the transient enzyme-bound species using stopped-flow spectrophotometry. The binding event was monitored by the intrinsic protein fluorescence change upon sugar substrate binding, as observed in the equilibrium binding experiments. Representative time traces for glucose and 2-deoxyglucose binding to WT GK are shown in panels A and B of Figure 3, respectively, and glucose binding to GK Y214C is shown in Figure 3C.

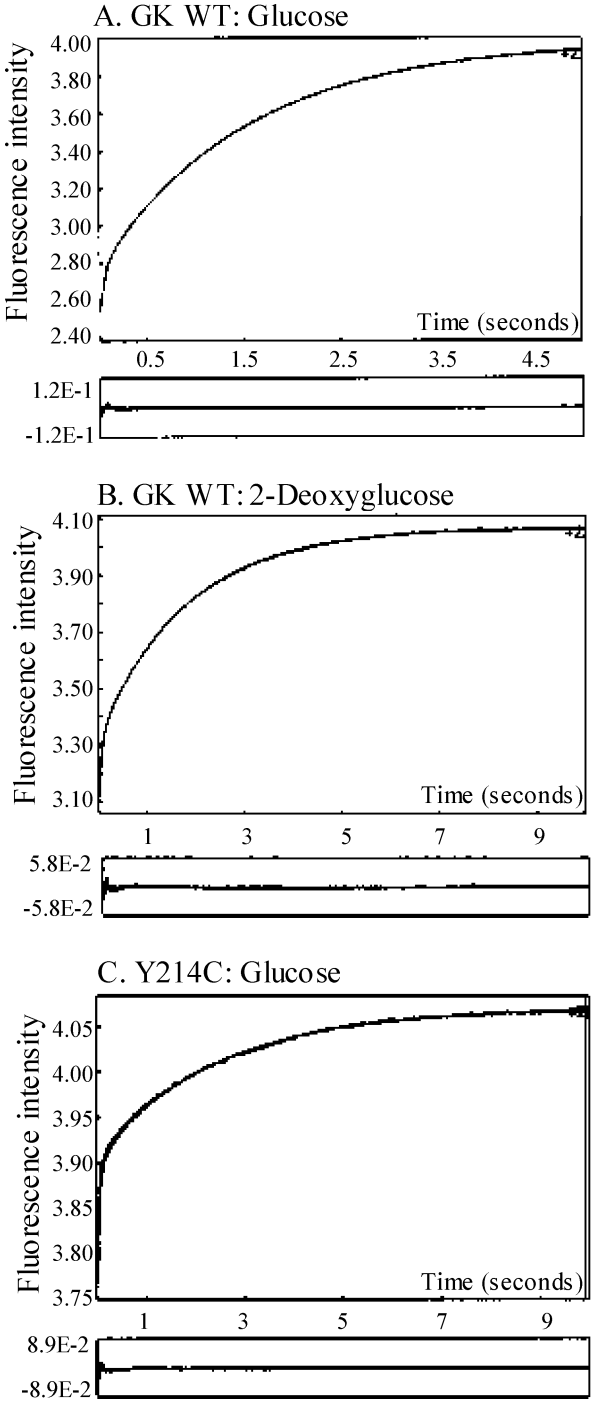

FIGURE 3: Representative stopped-flow transient kinetics observed for sugar substrates with human GK. All reactions were carried out in 50 mM HEPES buffer (pH 8.0) containing 25 mM KCl and 2 mM DTT at 25 °C. The protein fluorescence was monitored using a 320 nm cutoff filter upon excitation at 290 nm. (A) Reaction of 15 mM glucose with 9.6 μM WT GK. (B) Reaction of 150 mM 2-deoxyglucose with 7.7 μM WT GK. (C) Reaction of 0.5 mM glucose with 9.6 μM Y214C. The time traces were fit to a double-exponential equation (eq 2). Below each graph is the residual error with biphasic curve fitting.

The transient kinetic traces of GK exhibited biphasic behavior suggesting two kinetically distinguishable events. The observed rate constant for the first phase, k_{obs1}, was linearly dependent on the sugar substrate concentration, while

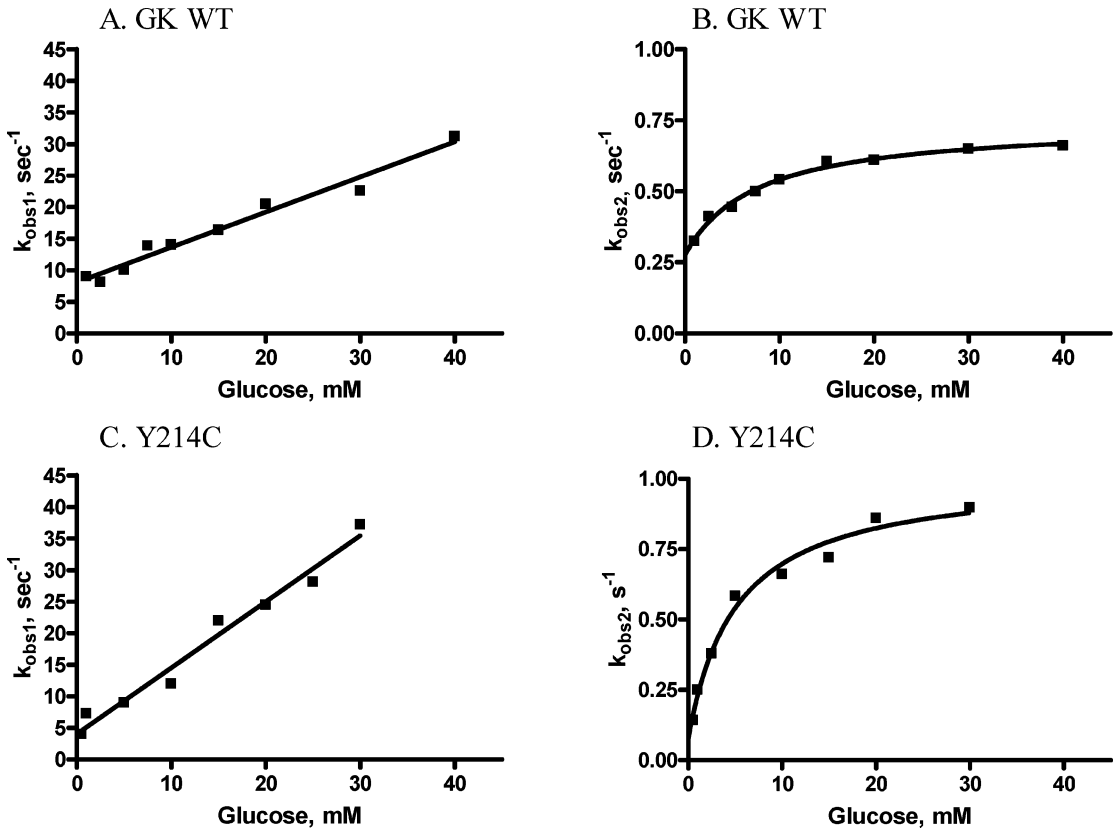

FIGURE 4: Representative fits of observed rate constants of glucose binding to WT GK (A and B) and Y214C (C and D). (A) Plot of k_{obs1} vs the concentration of glucose binding to WT GK fit to eq 3. (B) Plot of k_{obs2} vs the concentration of glucose binding to WT GK fit to eq 4. (C) Plot of k_{obs1} vs the concentration of glucose binding to Y214C fit to eq 3. (D) Plot of k_{obs2} vs the concentration of glucose binding to Y214C fit to eq 4.

the second-phase rate constant, k_{obs2}, exhibited a hyperbolic dependence on the substrate concentration (Figure 4). For WT GK, the amplitude for the first phase (A_1) was relatively small at ~25% of the total fluorescence change. These results suggest that the first phase describes a bimolecular binding event with a small perturbation of enzyme conformation, and the second phase involves a large enzyme conformational change. This two-step binding process is shown in the scheme below, where E* and E represent two enzyme conformations and S is the substrate.

$$E^* + S \underset{k_{-1}}{\overset{k_1}{\rightleftharpoons}} E^*\cdot S \underset{k_{-2}}{\overset{k_2}{\rightleftharpoons}} E\cdot S$$

Under pseudo-first-order conditions ($S \gg E$), k_{obs1} and k_{obs2} are related to the microscopic rate constants k_1, k_{-1}, k_2, and k_{-2} by eqs 3 and 4 (*23*):

$$k_{obs1} = k_{-1} + k_1 S \tag{3}$$

$$k_{obs2} = k_{-2} + \frac{k_2 S}{K_s + S} \tag{4}$$

where

$$K_s = k_{-1}/k_1 \tag{5}$$

The rate constants k_1 and k_{-1} for the first step binding were obtained by fitting k_{obs1} to eq 3. For the second step of the enzyme conformational change, rate constants k_2 and k_{-2} were determined by fitting k_{obs2} to eq 4. K_s was fit as a variable and was within 2-fold to the calculated value based on eq 5. The derived microscopic rate constants are listed in part A of Table 3 for WT GK and part B for Y214C.

For WT GK, the transient kinetic analysis indicated that the enzyme conformational change induced by glucose binding was a slow and reversible process with a k_2/k_{-2} of 1.6. The most significant difference between glucose and 2-deoxyglucose in the substrate binding to WT GK was the 15-fold lower on rate k_1 with 2-deoxyglucose, while the rates for the subsequent enzyme conformational change were similar.

Activating mutation Y214C exhibited altered transient kinetics for glucose binding. The amplitude for the first phase (A_1) was ~50% of the total fluorescence change. The microscopic rate constants changed by 2−4-fold in favor of glucose binding to Y214C. With 2-deoxyglucose as the substrate for Y214C, only k_2 was increased by 10-fold, while the remaining microscopic rate constants were unchanged compared to those of WT GK. For Y214C, both glucose and 2-deoxyglucose shifted the equilibrium between E*·S and E·S with similar k_2/k_{-2} ratios of 12 and 10, respectively, despite differences in individual rate constants.

The equilibrium binding affinity K_D is the overall combination of the microscopic kinetic constants of the multiple binding steps as described by eq 6 (*24*). The K_D calculated from transient kinetic data fitting was within 2-fold of the experimental K_D determined by fluorescence titration (Table 3).

$$K_D = \frac{k_{-1}}{k_1}\frac{k_{-2}}{k_2 + k_{-2}} \tag{6}$$

Table 3: Microscopic Rate Constants Associated with Binding of Substrate to (A) WT GK and (B) Y214C and Solvent Isotope Effects (SIE) Using Glucose as the Substrate

parameter	glucose (H_2O)	glucose (D_2O)	SIE, glucose (H_2O/D_2O)	2-deoxyglucose (H_2O)
		(A) WT GK		
k_1 (M^{-1} s^{-1})	557 ± 36	541 ± 66	1.0 ± 0.1	37 ± 3
k_{-1} (s^{-1})	8.1 ± 0.7	14 ± 1	0.58 ± 0.11	13 ± 1
k_2 (s^{-1})	0.45 ± 0.02	0.71 ± 0.04	0.63 ± 0.07	0.28 ± 0.03
k_{-2} (s^{-1})	0.28 ± 0.02	0.091 ± 0.010	3.1 ± 0.1	0.36 ± 0.01
k_2/k_{-2}	1.6 ± 0.1	7.8 ± 0.9		0.78 ± 0.09
K_D(calc)[a] (mM)	5.6 ± 0.8	2.9 ± 0.6		198 ± 31
		(B) Y214C		
k_1 (M^{-1} s^{-1})	1050 ± 64	1140 ± 59	0.92 ± 0.08	32 ± 4
k_{-1} (s^{-1})	4.7 ± 1.2	5.1 ± 1.0	0.92 ± 0.30	18 ± 1
k_2 (s^{-1})	0.94 ± 0.05	0.89 ± 0.05	1.1 ± 0.1	2.8 ± 0.5
k_{-2} (s^{-1})	0.078 ± 0.014	0.071 ± 0.015	1.1 ± 0.3	0.27 ± 0.01
k_2/k_{-2}	12 ± 2	12 ± 3		10 ± 2
K_D(calc)[a] (mM)	0.34 ± 0.11	0.33 ± 0.10		50 ± 11

[a] The K_D value is calculated on the basis of eq 6.

Table 4: Summary of Steady-State Kinetic Parameters Obtained from Kinetic Simulation

parameter	WT GK with glucose (H_2O)	WT GK with 2-deoxyglucose (H_2O)	WT GK with glucose (D_2O)	Y214C with glucose (H_2O)
$K_{0.5}$ (mM)				
simulation	9	178	5	3.2
experimental value	7.2 ± 0.2	153 ± 19	5.7 ± 0.2	2.2 ± 0.1
Hill slope				
simulation	1.5	1.1	1.3	1.3
experimental value	1.7 ± 0.1	1.1 ± 0.1	1.3 ± 0.1	1.2 ± 0.1

KINSIM Simulations. Because of the difficulty in directly measuring the rate constants of the active form E in glucose binding (k_3 and k_{-3}) and its isomerization (k_{relax}) under the current experimental settings, these parameters were assigned values in the simulation based on two assumptions. First, the E form should bind glucose at a significantly higher affinity. For WT GK, the K_D (k_{-3}/k_3) was set at 0.2 mM, approximately 20-fold lower than the equilibrium dissociation constant of 4.5 mM. This value is similar to the measured K_D of 0.1 mM for yeast HK with glucose (V. Heredia and S. Sun, unpublished results). This is a reasonable assumption since the active site in the E·glucose closed form is nearly identical to that in yeast HK (*10*, *11*). The k_3 must be large enough to support the observed enzyme turnover such that $k_3S \gg k_{cat}$ (38 s^{-1}). Thus, k_3 was set at 20 000 M^{-1} s^{-1}. With an S of 50 mM, k_3S is 1000 s^{-1}, a value significantly larger than k_{cat}. As a result, the k_{-3} value was calculated as 5 s^{-1}. For Y214C, k_3 and k_{-3} were set at 20 000 M^{-1} s^{-1} and 1 s^{-1}, respectively. The K_D (k_{-3}/k_3) for Y214C is now 0.05 mM, approximately 10−20-fold lower than the equilibrium dissociation constant of 0.67 mM.

Second, the apo form E to E* conversion is an irreversible process assuming E* is thermodynamically favored. In addition, the k_{relax} (E to E*) should be higher than k_{-2} (E· glucose to E*·glucose) because glucose enhances the stability of the enzyme in complex form (E·glucose). For WT GK, the k_{relax} was set at 1 s^{-1} for both glucose and 2-deoxyglucose as the substrate. Because the enzyme is more stable in D_2O for WT (k_{-2} = 0.091 s^{-1}) and Y214C (k_{-2} = 0.078 s^{-1}) than WT GK in H_2O (k_{-2} = 0.28 s^{-1}), k_{relax} was defined as 0.2 s^{-1} for both WT in D_2O and Y214C.

Table 4 summarizes the simulated results of $K_{0.5}$ and the Hill slope in comparison to the experimentally measured values, which showed close agreement for all the case studies. The slightly greater simulated $K_{0.5}$ values versus the measured ones may be due in part to the simplification of combining ATP binding, catalysis, and product release into one step. The effect of the simplification was to provide one fewer form of the enzyme with glucose bound and could lead to an underestimate of the fraction of enzyme with glucose bound, thereby slightly increasing the $K_{0.5}$ value in the simulation relative to the measured value.

DISCUSSION

The underlying mechanism for the sigmoidal kinetics of GK has been a primary interest in the study of this monomeric enzyme. The traditional concerted model for cooperative kinetics does not apply to a monomeric enzyme with a single substrate-binding site. Recently, the possibility of two glucose binding sites in GK was raised (*25*). In our study, the equilibrium binding of glucose to GK in the absence of ATP displays a hyperbolic dependence on glucose concentration, consistent with a single glucose-binding site that was also observed in the crystal structure of GK (*10*, *14*, *15*). Thus, the positive cooperativity with glucose in GK appears to originate from a kinetic property. Several kinetic models have been proposed to explain the cooperative kinetics for GK, such as a mnemonical model (*26*) and a slow transition model (*27*). The common feature in these models is that the enzyme exists in two distinct forms that interconvert by substrate binding. The enzyme conformational transition is slow relative to the catalytic step, and the two enzyme forms do not reach equilibrium at the steady state, leading to cooperative kinetics with the substrate concentration. The crystal structures of GK in its inactive form (apo-GK) and active form (GK·glucose·activator complex) demonstrated large conformational changes between the two forms (*10*, *28*). In the apo form, the enzyme

displays a "wide-open" conformation without a definitive allosteric site. Once GK forms a complex with glucose and the activator, the enzyme adopts a more compact form with well-defined sites for both glucose and the activator, mainly through substantial reorganization of the small domain (*10*). To investigate the linkage between the structural change in GK and its kinetic profile, we studied the transient kinetics of glucose binding in relation to the glucose-induced conformational change in GK, and furthermore the kinetic basis of GK activation by mutation at the allosteric site.

Sequential Binding of Glucose and ATP to Human β-Cell WT GK. Glucose cooperativity in GK makes steady-state kinetic analyses of the enzyme's kinetic mechanism difficult. To avoid this challenge, Monasterio et al. used the noncooperative substrate 2-deoxyglucose to demonstrate an ordered bi-bi mechanism for rat liver GK in which the sugar substrate binds prior to Mg·ATP and Mg·ADP is released last (*29*). However, isotope-exchange measurements performed at equilibrium in an earlier report suggested a small portion of random behavior, although no binary E·ATP complex could be detected (*30*). In this study using differential scanning calorimetry, a shift in the thermal midpoint of transition of GK observed in the presence of glucose and the absence of a shift in the thermal midpoint of transition in the presence of ATP suggest that substrate binding occurs via sequential events with glucose binding first followed by the cofactor ATP. As no cofactor binding was observed in the absence of glucose, glucose binding must be a prerequisite for ATP binding.

Kinetic Characterization of the Glucose-Induced Conformational Change in WT GK. Binding of glucose to GK induced a global alteration in the enzyme conformation that caused the changes in its intrinsic protein fluorescence. The observed biphasic transient kinetics is consistent with a two-step reversible binding mechanism of an initial bimolecular binding event followed by a slow enzyme isomerization step. This biphasic nature of glucose binding was previously observed in rat liver GK (*27*). Because of technical limitations on the time scale for monitoring the reaction, the previous study was performed in 5 or 30% glycerol to slow transient kinetics. Only the kinetics for the slow second phase was determined. Our study confirms the presence of biphasic kinetics and also extends the current understanding by measuring binding rates at very fast time scales in the absence of glycerol. The difference in the reported transient rate constants is likely due to the experimental conditions and the time scale used to measure the kinetics.

Coupled with the structural evidence for a large conformational change in GK upon glucose binding (*10*), a kinetic model describing the substrate binding and subsequent turnover is proposed in Scheme 1. A thermodynamically favored apo-form E* initially binds glucose to form the E*·glucose binary complex. This apoenzyme is essentially inactive for catalysis, although it can bind glucose weakly with a slow on rate of 557 M^{-1} s^{-1} and a weak affinity of 14.5 mM (k_{-1}/k_1). Glucose binding induces a domain closure in wide-open form E* to closed form E. The interconversion between E*·glucose and E·glucose appears to be slow with a k_2 of 0.45 s^{-1} and a k_{-2} of 0.28 s^{-1}, most likely due to a large kinetic energy barrier between the two conformations. The second substrate, ATP, is then able to bind to the E·glucose complex and transfer P_i to glucose. After the products are released, the apoenzyme exists in the active form, E, which can either relax back to the thermodynamically favored form, E* (k_{relax}), or bind glucose if available to re-enter the catalytic cycle (k_3 and k_{-3}). The ratio of inactive form (E*) to active form (E) is determined by these two competing events. At low glucose concentrations, the majority of the free enzyme is in the inactive form (E*); thus, the overall enzyme activity is very low. When the glucose concentration is sufficiently high, glucose retains the enzyme in the active form (E). The shift in the ratio of enzyme isoforms toward active form E caused by glucose gives rise to the observed positive cooperativity with glucose.

The glucose-induced enzyme conformational change is 85-fold slower than the rate of glucose turnover at saturating substrate concentrations ($k_2 = 0.45$ s^{-1} vs $k_{cat} = 38$ s^{-1}), which implies that the conversion from E* to E occurs outside the catalytic cycle of GK. Upon close examination of the time course of the steady-state kinetics for glucose turnover, a lag phase is observed when assays are initiated by enzyme but not when enzyme and glucose are preincubated before addition of ATP to initiate the reaction (Supporting Information). Because binding of glucose to GK primes the enzyme to enter the catalytic cycle, a lag phase is apparent especially at low glucose concentrations, which eventually decreases as the glucose concentration is increased. This lag phase is likely not due to the coupled-assay system as addition of excess coupling enzyme had no effects on the lag phase and the steady-state rates.

Additional supporting evidence for the kinetic basis of positive cooperativity of GK comes from the transient kinetic analysis of the noncooperative substrate 2-deoxyglucose. The biphasic transient kinetics observed with 2-deoxyglucose suggests that the two-step event of substrate binding and consequent enzyme conformational change still occurs. While the microscopic rate constants for the enzyme isomerization step (k_2 and k_{-2}) are essentially the same as those for glucose, the initial binding step is now dramatically decreased with a 15-fold lower bimolecular rate constant, k_1. The intrinsic slow binding of 2-deoxyglucose to GK may lead to the reduced sigmoidal kinetics.

There are significant solvent isotope effects on glucose binding as well as glucose turnover in WT GK. GK has a 2.4-fold higher binding affinity for glucose in D_2O than in H_2O. The detailed transient kinetic analysis shows that the D_2O effects come from both the initial glucose binding and subsequent enzyme conformational change. The glucose on rate, k_1, is not changed, whereas the glucose off rate, k_{-1}, is increased from 8.1 to 14 s^{-1}. This is offset by a shift in the equilibrium between E and E* toward the active form (E) in D_2O by the combination of a 1.6-fold increase in k_2 and a 3-fold decrease in the reverse step, k_{-2} ($k_2/k_{-2} = 1.6$ in H_2O vs 7.8 in D_2O). Thus, the active form (E) is more stable in D_2O. The net result is that the overall glucose binding affinity is increased. Furthermore, the favored equilibrium toward the active enzyme (E) in D_2O makes the positive cooperativity by glucose less significant (Hill slope of 1.3 in D_2O vs a value of 1.7 in H_2O). These observations support the model of a kinetic origin for the positive cooperativity with glucose in WT GK.

In contrast, HKs do not exhibit positive cooperativity with glucose (*12*). The crystal structures of yeast HK indicate a conformational change from an open to a closed form

induced by glucose binding (*11*, *31*−*33*). However, the open to closed conformational change in HK involves a degree of protein domain movement smaller than that observed for GK. Stopped-flow studies suggest that binding of glucose to yeast HK and the subsequent enzyme conformational changes are completed within 1 ms, consistent with an earlier report of a nanosecond time scale (*34*). Thus, the slow transient kinetics in GK aligns with its dramatic structural change, which is directly linked to the enzyme's cooperative behavior.

Kinetic Basis of GK Activation by Allosteric Site Mutation Y214C. Like WT GK, Y214C displays biphasic kinetics, suggesting that the two-step binding mechanism also applies to Y214C. The increased glucose affinity for Y214C (K_D = 0.67 mM for Y214C and K_D = 4.5 mM for WT) can be attributed to altered kinetics in both steps of substrate binding. In the first step of bimolecular binding, formation of the E*·glucose complex (k_1) is accelerated by 2-fold, and the dissociation (k_{-1}) was attenuated by nearly 2-fold in Y214C. In the following step, the enzyme isomerization is shifted toward the active form (E) with a k_2/k_{-2} ratio of 12 in Y214C versus a ratio of 1.6 in WT GK. As a result, the glucose binding affinity is increased while its cooperativity is decreased in Y214C. These two parallel effects are similar to the deuterium solvent isotope effects for WT. Interestingly, small solvent isotope effects were observed in binding of glucose to Y214C, suggesting no further stabilization of the active form (E) in D_2O. With either glucose or 2-deoxyglucose as the substrate, the k_2/k_{-2} ratio was 10−12 and 0.8−1.6 for Y214C and WT, respectively. Therefore, the equilibrium between the two enzyme conformations (k_2/k_{-2}) is not significantly altered in the presence of different sugar substrates.

Overall, the Y214C mutation shows both enhanced initial glucose binding and a conformational change to the active form of the enzyme. The observed kinetic changes for Y214C may result from structural changes in the apoenzyme that favor glucose binding. One hypothesis is that the Y214C mutation could lead to a more compact overall structure for the apoenzyme that shows some features of the closed, active form. A better understanding of the structural consequences of Y214C would be revealed by its crystal structure.

Possible Activation Mechanism for Small Molecule Activators. Recently, small molecules that bind to the allosteric site were discovered and shown to enhance GK activity mainly by decreasing the $K_{0.5}$ for glucose like the activating mutations (*10*, *14*, *15*, *28*). These GK activators stimulate insulin secretion in β-cells and suppress glucose production in the liver. They lower blood glucose levels in normal and diabetic animals and provide a promising therapeutic approach for treating type 2 diabetes (*35*−*38*). The activation mechanism by small molecules is not well understood. On the basis of the findings for naturally occurring activating mutation Y214C, some explanations for small molecule activation can be proposed here. First, crystal structures of GK show that the allosteric site is absent in the apoenzyme, suggesting that activators only bind to the closed form enzyme induced by glucose binding. In the absence of glucose, the activator was unable to bind to GK (data not shown). Unlike Y214C, which demonstrated a faster on rate k_1 and slower off rate k_{-1} for glucose binding (Scheme 1), activators should not alter the first binding event because activator binding occurs only after glucose binds, and the enzyme conformation has changed to E·glucose. Second, the activator likely shifts the equilibrium between the two enzyme forms toward the active form (E) by a combination of increasing forward rate k_2 and decreasing reverse step k_{-2}, which is like the Y214C effect (V. Heredia and S. Sun, unpublished results). As a result, the active form enzyme (E) is stabilized in the presence of activators, leading to an increased glucose binding affinity. This overall effect would be consistent with lower $K_{0.5}$ and Hill slope values observed for glucose when the activator is present (*10*, *14*).

Quantitative analysis of the kinetic data by KINSIM simulations shows that the cooperativity of GK can be explained by the model proposed in Scheme 1, in which the slow conformational change associated with binding of glucose to GK results in its sigmoidal kinetics. The simulations also demonstrate that the slow binding of 2-deoxyglucose leads to nearly hyperbolic kinetics with GK. Furthermore, reduced Hill slope values were observed in simulations for binding of glucose to WT GK in D_2O and to Y214C, consistent with the experimental results. On the basis of the experimental observations and simulations for the four sets of kinetic values, the Hill slope can be modulated by the on rate for binding of sugar substrate to GK, k_1 (e.g., 2-deoxyglucose), and/or the conformational change between the inactive and active forms of the enzyme, k_2, k_{-2}, and k_{relax} (e.g., D_2O and Y214C). Therefore, the cooperativity of GK is a kinetic behavior that is mediated by the glucose-induced conformational change in GK.

Combining these kinetic details with enzyme structural analysis suggests that GK is a highly dynamic enzyme whose kinetic profiles can be interpreted in relation to its structural changes. Allosteric site activating mutation Y214C results in enhanced initial glucose binding to the apoenzyme and facilitation of the subsequent enzyme conformational change to the active form. The underlying mechanism for GK activation by small molecule activators may share some features of the activating mutation, such as shifting the equilibrium of the enzyme conformation toward the active form. The critical role of glucokinase as a glucose sensor in glucose homeostasis and the possibility of modulating enzyme activity through small molecule activators make the enzyme a highly attractive and feasible drug target for the treatment of type 2 diabetes.

ACKNOWLEDGMENT

We thank Janice Chin for kindly providing the WT GK clone, Tom Carlson, Erin Garcia, and Jon Almaden for their expert technical support in protein purification and assay development, and Jim Nonomiya for technical assistance with QTOF-MS. We also thank Cris Lewis, Steve Grant, and Jen Digits for critical reading of the manuscript and insightful discussion.

SUPPORTING INFORMATION AVAILABLE

Figures from the DSC experiment and single-exponential fits for binding of glucose and 2-deoxyglucose to WT GK and Y214C and time courses using the PK/LDH coupled assay in the presence and absence of GK incubation with glucose. This material is available free of charge via the Internet at http://pubs.acs.org.

REFERENCES

1. Matschinsky, F. M. (2005) Glucokinase, glucose homeostasis, and diabetes mellitus, *Curr. Diabetes Rep. 5*, 171−176.
2. Matschinsky, F. M. (1990) Glucokinase as glucose sensor and metabolic signal generator in pancreatic β-cells and hepatocytes, *Diabetes 39*, 647−652.
3. Cardenas, M. L. (1995) *Glucokinase: Its Regulation and Role in Liver Metabolism*, R. G. Landes, Austin, TX.
4. Agius, L., Peak, M., Newgard, C. B., Gomez-Foix, A. M., and Guinovart, J. J. (1996) Evidence for a role of glucose-induced translocation of glucokinase in the control of hepatic glycogen synthesis, *J. Biol. Chem. 271*, 30479−30486.
5. Matschinsky, F., Liang, Y., Kesavan, P., Wang, L., Froguel, P., Velho, G., Cohen, D., Permutt, M. A., Tanizawa, Y., Jetton, T. L., Niswender, K., and Magnuson, M. A. (1993) Glucokinase as pancreatic β-cell glucose sensor and diabetes gene, *J. Clin. Invest. 92*, 2092−2098.
6. Glaser, B., Kesavan, P., Heyman, M., Davis, E., Cuesta, A., Buchs, A., Stanley, C. A., Thornton, P. S., Permutt, M. A., Matschinsky, F. M., and Herold, K. C. (1998) Familial hyperinsulinism caused by an activating glucokinase mutation, *N. Engl. J. Med. 338*, 226−230.
7. Christesen, H. B., Jacobsen, B. B., Odili, S., Buettger, C., Cuesta-Munoz, A., Hansen, T., Brusgaard, K., Massa, O., Magnuson, M. A., Shiota, C., Matschinsky, F. M., and Barbetti, F. (2002) The second activating glucokinase mutation (A456V): Implications for glucose homeostasis and diabetes therapy, *Diabetes 51*, 1240−1246.
8. Cuesta-Munoz, A. L., Huopio, H., Otonkoski, T., Gomez-Zumaquero, J. M., Nanto-Salonen, K., Rahier, J., Lopez-Enriquez, S., Garcia-Gimeno, M. A., Sanz, P., Soriguer, F. C., and Laakso, M. (2004) Severe persistent hyperinsulinemic hypoglycemia due to a de novo glucokinase mutation, *Diabetes 53*, 2164−2168.
9. Bontemps, F., Hue, L., and Hers, H. G. (1978) Phosphorylation of glucose in isolated rat hepatocytes. Sigmoidal kinetics explained by the activity of glucokinase alone, *Biochem. J. 174*, 603−611.
10. Kamata, K., Mitsuya, M., Nishimura, T., Eiki, J., and Nagata, Y. (2004) Structural basis for allosteric regulation of the monomeric allosteric enzyme human glucokinase, *Structure 12*, 429−438.
11. Bennett, W. S., Jr., and Steitz, T. A. (1980) Structure of a complex between yeast hexokinase A and glucose. I. Structure determination and refinement at 3.5 Å resolution, *J. Mol. Biol. 140*, 183−209.
12. Wilson, J. E. (1995) Hexokinases, *Rev. Physiol. Biochem. Pharmacol. 126*, 65−198.
13. Aleshin, A. E., Zeng, C., Bartunik, H. D., Fromm, H. J., and Honzatko, R. B. (1998) Regulation of hexokinase I: Crystal structure of recombinant human brain hexokinase complexed with glucose and phosphate, *J. Mol. Biol. 282*, 345−357.
14. Grimsby, J., Sarabu, R., Corbett, W. L., Haynes, N. E., Bizzarro, F. T., Coffey, J. W., Guertin, K. R., Hilliard, D. W., Kester, R. F., Mahaney, P. E., Marcus, L., Qi, L., Spence, C. L., Tengi, J., Magnuson, M. A., Chu, C. A., Dvorozniak, M. T., Matschinsky, F. M., and Grippo, J. F. (2003) Allosteric activators of glucokinase: Potential role in diabetes therapy, *Science 301*, 370−373.
15. Brocklehurst, K. J., Payne, V. A., Davies, R. A., Carroll, D., Vertigan, H. L., Wightman, H. J., Aiston, S., Waddell, I. D., Leighton, B., Coghlan, M. P., and Agius, L. (2004) Stimulation of hepatocyte glucose metabolism by novel small molecule glucokinase activators, *Diabetes 53*, 535−541.
16. Dunten, P., Swain, A., Kammlott, U., Crowther, R., Lukacs, C. M., Levin, W., Reik, L., Grimsby, J., Corbett, W. L., Magnuson, M. A., Matschinsky, F. M., and Grippo, J. F. (2004) Crystal structure of human liver glucokinase bound to a small molecule activator, in *Glucokinase and glycemic disease: from basics to novel therapeutics* (Matschinsky, F. M., and Magnuson, M. A., Eds.) Karger, Basel, Switzerland.
17. Nishi, S., Stoffel, M., Xiang, K., Shows, T. B., Bell, G. I., and Takeda, J. (1992) Human pancreatic β-cell glucokinase: cDNA sequence and localization of the polymorphic gene to chromosome 7, band p 13, *Diabetologia 35*, 743−747.
18. Bradford, M. M. (1976) A rapid and sensitive method for the quantitation of microgram quantities of protein utilizing the principle of protein-dye binding, *Anal. Biochem. 72*, 248−254.
19. Schowen, K. B., and Schowen, R. L. (1982) Solvent isotope effects of enzyme systems, *Methods Enzymol. 87*, 551−606.
20. Northrop, D. B. (1982) Deuterium and tritium kinetic isotope effects on initial rates, *Methods Enzymol. 87*, 607−625.
21. Barshop, B. A., Wrenn, R. F., and Frieden, C. (1983) Analysis of numerical methods for computer simulation of kinetic processes: Development of KINSIM: A flexible, portable system, *Anal. Biochem. 130*, 134−145.
22. Sturtevant, J. M. (1987) Biochemical applications of differential scanning calorimetry, *Annu. Rev. Phys. Chem. 38*, 463−488.
23. Fersht, A. (1999) *Structure and Mechanism in Protein Science*, W. H. Freeman and Co., New York.
24. Lin, S. X., and Neet, K. E. (1990) Demonstration of a slow conformational change in liver glucokinase by fluorescence spectroscopy, *J. Biol. Chem. 265*, 9670−9675.
25. Agius, L., and Stubbs, M. (2000) Investigation of the mechanism by which glucose analogues cause translocation of glucokinase in hepatocytes: Evidence for two glucose binding sites, *Biochem. J. 346* (Part 2), 413−421.
26. Cornish-Bowden, A., and Storer, A. C. (1986) Mechanistic origin of the sigmoidal rate behaviour of rat liver hexokinase D ('glucokinase'), *Biochem. J. 240*, 293−296.
27. Neet, K. E., Keenan, R. P., and Tippett, P. S. (1990) Observation of a kinetic slow transition in monomeric glucokinase, *Biochemistry 29*, 770−777.
28. Efanov, A. M., Barrett, D. G., Brenner, M. B., Briggs, S. L., Delaunois, A., Durbin, J. D., Giese, U., Guo, H., Radloff, M., Gil, G. S., Sewing, S., Wang, Y., Weichert, A., Zaliani, A., and Gromada, J. (2005) A novel glucokinase activator modulates pancreatic islet and hepatocyte function, *Endocrinology 146*, 3696−3701.
29. Monasterio, O., and Cardenas, M. L. (2003) Kinetic studies of rat liver hexokinase D ('glucokinase') in non-cooperative conditions show an ordered mechanism with MgADP as the last product to be released, *Biochem. J. 371*, 29−38.
30. Gregoriou, M., Trayer, I. P., and Cornish-Bowden, A. (1981) Isotope-exchange evidence for an ordered mechanism for rat-liver glucokinase, a monomeric cooperative enzyme, *Biochemistry 20*, 499−506.
31. Bennett, W. S., Jr., and Steitz, T. A. (1978) Glucose-induced conformational change in yeast hexokinase, *Proc. Natl. Acad. Sci. U.S.A. 75*, 4848−4852.
32. Bennett, W. S., Jr., and Steitz, T. A. (1980) Structure of a complex between yeast hexokinase A and glucose. II. Detailed comparisons of conformation and active site configuration with the native hexokinase B monomer and dimer, *J. Mol. Biol. 140*, 211−230.
33. Steitz, T. A. (1971) Structure of yeast hexokinase-B. I. Preliminary X-ray studies and subunit structure, *J. Mol. Biol. 61*, 695−700.
34. Maity, H., Maiti, N. C., and Jarori, G. K. (2000) Time-resolved fluorescence of tryptophans in yeast hexokinase-PI: Effect of subunit dimerization and ligand binding, *J. Photochem. Photobiol., B 55*, 20−26.
35. Zelent, D., Najafi, H., Odili, S., Buettger, C., Weik-Collins, H., Li, C., Doliba, N., Grimsby, J., and Matschinsky, F. M. (2005) Glucokinase and glucose homeostasis: Proven concepts and new ideas, *Biochem. Soc. Trans. 33*, 306−310.
36. Leighton, B., Atkinson, A., and Coghlan, M. P. (2005) Small molecule glucokinase activators as novel anti-diabetic agents, *Biochem. Soc. Trans. 33*, 371−374.
37. Sarabu, R., and Grimsby, J. (2005) Targeting glucokinase activation for the treatment of type 2 diabetes A status review, *Curr. Opin. Drug Discovery Dev. 8*, 631−637.
38. Al-Hasani, H., Tschop, M. H., and Cushman, S. W. (2003) Two birds with one stone: Novel glucokinase activator stimulates glucose-induced pancreatic insulin secretion and augments hepatic glucose metabolism, *Mol. Interventions 3*, 367−370.

BI060253Q